

NANO EXPRESS

Open Access



# Supramolecular Gel-Templated In Situ Synthesis and Assembly of CdS Quantum Dots Gels

Lili Zhu<sup>1,3†</sup>, Jie He<sup>1†</sup>, Xiaoliang Wang<sup>2</sup>, Dawei Li<sup>2</sup>, Haibing He<sup>2</sup>, Lianbing Ren<sup>1</sup>, Biwang Jiang<sup>1</sup>, Yong Wang<sup>1\*</sup>, Chao Teng<sup>1\*</sup>, Gi Xue<sup>2\*</sup> and Huchun Tao<sup>3\*</sup>

## Abstract

Although many studies have attempted to develop strategies for spontaneously organizing nanoparticles (NPs) into three-dimensional (3D) geometries, it remains a fascinating challenge. In this study, a method for in situ synthesis and self-assembly of a CdS quantum dots (QDs) gel using a Cd supramolecular gel as a scaffold was demonstrated. During the QDs formation process, the Cd ions that constituted the Cd gels served as the precursors of the CdS QDs, and the oleic acid (OA) that ligated with the Cd in the supramolecular gels was capped on the surface of the CdS QDs in the form of carboxylate. The OA-stabilized CdS QDs were in situ synthesized in the entangled self-assembled fibrillar networks (SAFIN) of the Cd gels through reactions between the gelator and H<sub>2</sub>S. As a result, the QDs exactly replicated the framework of the SAFIN in the CdS QD gels instead of simply assembling along the SAFIN of the supramolecular gels. Moreover, the CdS QDs showed extraordinary sensitivity in the fluorescence detection of IO<sub>4</sub><sup>-</sup> anions. The facile one-step method developed here is a new approach to assembling nanostructured materials into 3D architectures and has general implications for the design of low molecular mass gelators to bring desired functionality to the developed supramolecular gels.

**Keywords:** Quantum dots, Fluorescent probe, Self-assembled fibrillar networks, Template synthesis

## Background

Organized assemblies of nanoparticles (NPs) with diversified structures have received much attention because they combine both the unique size-dependent physical properties of individual NPs and the collective physical properties that can optimize and extend their applications in optical and electronic fields [1–10]. Various approaches have been developed to fabricate NPs into

an ordered assembly, including self-assembly induced by cold treatment, solvent evaporation, and templated organization by biomolecules or lyotropic liquid crystals [11–29]. Despite these studies, developing a facile and efficient method to self-assemble NPs into ordered structures is still challenging, especially for three-dimensional (3D) geometries [30–35].

Recently, there has been considerable interest in using supramolecular gels, which are gels derived from low molecular mass gelators, to assemble NPs into different structures [36–45]. Due to the tunability of the structure of these gelators, the entangled self-assembled fibrillar networks (SAFINs) formed by the self-aggregation of these small gelators are superior templates for assembling NPs into two- or three-dimensional architectures [46–50]. Although a large number of studies of the in situ synthesis and stabilization of inorganic NPs are focused on Si/TiO<sub>2</sub> NPs, an increasing number of studies have reported the ordered assembly of quantum dots (QDs) within a gel matrix [50–52]. Bardelang and Yu et

\* Correspondence: ywang@pkusz.edu.cn; tengc@pkusz.edu.cn; xuegi@nju.edu.cn; taohc@pkusz.edu.cn

†Equal contributors

<sup>1</sup>Guangdong Provincial Key Laboratory of Nano-Micro Material Research, School of Chemical Biology & Biotechnology, Peking University Shenzhen Graduate School, Shenzhen 518055, China

<sup>2</sup>Department of Polymer Science and Engineering, The School of Chemistry and Chemical Engineering, Key Laboratory of High Performance Polymer Materials and Technology (Nanjing University), Ministry of Education, The State Key Laboratory of Coordination Chemistry, Nanjing University, Nanjing 210093, China

<sup>3</sup>Key Laboratory for Heavy Metal Pollution Control and Reutilization, School of Environment and Energy, Peking University Shenzhen Graduate School, Shenzhen 518055, China

al. reported the preparation of QD-dipeptide nanocomposite gels using an ultrasound technique [50]. The CdSe/ZnS QDs were found to form along the peptide fibers due to multiple weak van der Waals interactions. Simmons and John et al. introduced a method to incorporate nanoparticles into the strands of a gel by linking small molecules through non-covalent interactions [53]. The immobilization of the super-paramagnetic ferrite nanoparticles and photochromic CdS QDs confers magnetic and/or luminescent properties on the gels. Lu et al. demonstrated the self-organization of porous CdS nanofibers with “pearl-necklace” architectures using a dicholesterol-based organogelator as a template [51]. However, due to the difficulty in designing low-molecule mass gelators and the lack of a detailed understanding of the how these small gelators aggregate, it is still difficult to fabricate NPs into ordered architectures. In addition, in most previous studies NPs were attached to the fibers during the assembly process by interactions between the functional groups of protecting ligands on the NPs and the gelators. Few studies have reported the formation of NPs gels with 3D networks in which the NPs self-assembled to form the actual SAFIN of the NPs gels rather than only being coated on the fibers of the supramolecular gels.

In this study, a one-step method for the in situ synthesis of CdS QD gels with 3D networks using a supramolecular Cd organogel as a scaffold was developed. The morphology and the structure of the obtained CdS gels were investigated using transmission electron microscopy (TEM), X-ray diffraction (XRD), UV-visible, and Fourier transform infrared spectroscopy (FT-IR). Finally, we demonstrated that the CdS gels could serve as fluorescent probes for the selective determination of trace levels of  $\text{IO}_4^-$  anions.

## Methods

### Chemicals and Materials

1-octadecene (ODE 90%), oleic acid (OA 90%), cadmium acetate ( $\text{Cd}(\text{OAc})_2 \cdot 2\text{H}_2\text{O}$  99.99 + %), and sodium sulfide (>98%) were purchased from Aldrich Chemical Co. All of the solvents were commercially available and distilled before use. All of the glassware was cleaned and rinsed with Milli-Q water, and then dried in an oven overnight before use.

### Preparation of Cadmium Organogel

The organogel was prepared following Shi's method [54]; 20 ml, 62.4 mmol ODE, 0.512 ml, 1.6 mmol OA, and 1.1064 g, 0.4 mmol cadmium acetate were mixed in a Schlenk flask. After degassing for 1 h at room temperature, the mixture was heated to 175 °C with constant stirring in nitrogen. The reaction proceeded at 175 °C for 1 h. Then the solution was left standing at room temperature to let

the gelator molecules self-associate to form networks. The gelator was made of Cd complexes ligated with OLA ( $\text{Cd}_2(\text{OOC}-(\text{CH}_2)_7-\text{CH}=\text{CH}-(\text{CH}_2)_7-\text{CH}_3)_4$ ), as shown in Fig. 1.

### Preparation of CdS QDs Networks

The in situ synthesis of the three-dimensional networks was carried out by exposing the cadmium supramolecular organogel to  $\text{H}_2\text{S}$  vapor, which was the source of the sulfur, at room temperature for 10 min. The  $\text{H}_2\text{S}$  was generated from the neutralization of a saturated solution of sodium sulfide with 2.5 mol/L sulfuric acid. The reaction system was then left to stand at room temperature for 1 day. A saffron yellow CdS QD gel was obtained.

### Characterization

Purified samples of the CdS QDs were characterized using TEM, UV-vis absorption spectra, FT-IR, XRD, and fluorescence spectra. Acetone and chloroform were used to wash away any extra reactants. Then, the yellow CdS QDs were dispersed in toluene or dimethyl sulfoxide before further measurement.

All of the TEM images were recorded using a JEOL JEM-2100 electron microscopy at an accelerating bias voltage of 200 kV. The samples for the TEM analysis were prepared by dipping standard carbon-coated copper grids into the sample solution. The TEM grids were withdrawn from the solution and allowed to dry under ambient atmosphere overnight. FT-IR was performed with a Vector 22 FT-IR Spectrometer. The sample solution was deposited dropwise onto a KBr disc. The FT-IR spectra of the CdS QDs were collected after the evaporation of the solvents. The background spectra of a clean KBr disc were collected under the same experimental conditions and subtracted from the sample spectra. The UV-vis spectra were recorded in 200–600 nm range using a UV-3600 spectrophotometer, and the samples were dispersed in toluene with different concentrations.

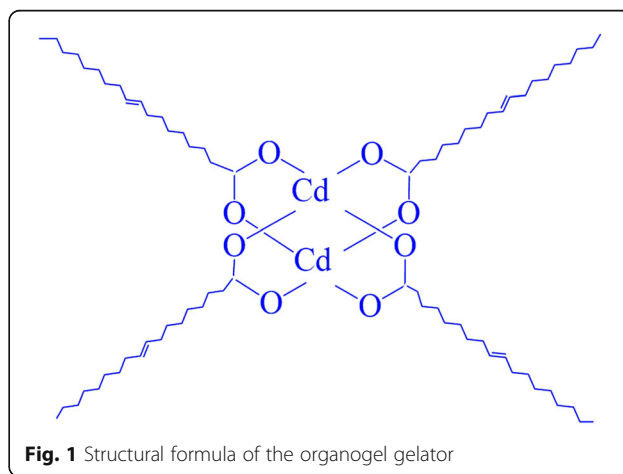


**Fig. 1** Structural formula of the organogel gelator

The fluorescence spectra were recorded with an Ls-55 fluorescence spectrometer from PE. The influence of the pH value and the concentration of CdS QDs on the fluorescence intensity were investigated. A phosphoric buffer solution (PBS) with a system pH value of around 7 was prepared by mixing  $\text{Na}_2\text{HPO}_4 \cdot 2\text{H}_2\text{O}$  and  $\text{NaH}_2\text{PO}_4 \cdot 2\text{H}_2\text{O}$ , and this solution was then used to tailor the PH of the sample solutions. The fluorescence intensity was recorded at 330 nm with an excitation wavelength of 273 nm. The XRD experiment was performed on a D8 ADVANCE X-ray powder diffractometer from Bruker AXS using CdS powder dried under a vacuum.

## Results and Discussion

During the gelation process, the small gelator molecules self-aggregated to form SAFINs through a combination of non-covalent interactions. Figure 2 shows the samples gelled from the low-molecular mass gelator abbreviated as G1, G2, and G3, which were taken out after they had gelled for 8, 24, and 72 h, respectively. G1, G2, and G3, as they were taken out at different stages of the gelation process, were in different states. G1 and G2 were liquids, whereas G3 was an organogel. At the molecular level, the binuclear dicadmium tetraoleate (in Fig. 1) was assembled to form 3D networks in G3. Samples G1, G2, and G3 were exposed to  $\text{H}_2\text{S}$  vapor to synthesize CdS QDs; the CdS samples obtained from G1, G2, G3 were abbreviated as Q1, Q2, and Q3, respectively. After reacting with  $\text{H}_2\text{S}$ , all of the gelator samples changed from transparent to yellow or saffron yellow, indicating the formation of CdS QDs. As shown in Fig. 2, yellow precipitates were observed at the bottom in Q1 and Q2, because the CdS QDs precipitated from the ODE. However, in Q3 a saffron yellow gel formed rather than a precipitate, indicating that CdS QDs assembled into 3D networks in Q3. The Q3 samples remained stable at room temperature.

The morphology of the CdS samples Q1, Q2, Q3 was studied by TEM, as shown in Fig. 3. Compared with the scattered structure of CdS in Q1 and Q2 (Fig. 3a, b), CdS gel sample Q3 had closely packed, networked structures (Fig. 3c). The TEM results demonstrated the existence of CdS QDs with network structures in Q3. Cadmium ions, which were constituents of the supramolecular gels, served as the precursors of CdS QDs. In addition, the formation of the gel in sample Q3 indicated the existence of interactions between OA-capped CdS QDs. Energy-dispersive X-ray spectroscopy (EDS) proved that Q3 was composed of Cd and S (Fig. 3d). Based on the EDS statistics, the molar ratio of Cd to S was 1:1.

FTIR was used to further investigate the interactions between OA and CdS QDs (shown in Fig. 4a). The absorptions at 2855 and 2934  $\text{cm}^{-1}$  were assigned to the symmetric and asymmetric stretching vibrations of C–H, respectively. The disappearance of peaks for carboxylic at 1710  $\text{cm}^{-1}$  and the appearance of peaks for carboxylate at 1627 and 1545  $\text{cm}^{-1}$  indicated that OA reacted with CdS QDs and formed carboxylate. The peak at 721  $\text{cm}^{-1}$  belonged to the rocking vibration of  $-\text{CH}_2$ . These FTIR results confirmed that OA was successfully capped on the surface of CdS QDs. OA, which ligated with Cd in G3, capped on the surface of CdS QDs in the form of carboxylate. According to these results and the packing model of G3 reported above, we propose that OA-capped CdS QDs were in situ formed in the SAFINs of the supramolecular gel template, and they kept the exact morphology of the network structures. In a swollen state, the intermolecular interactions between such CdS building blocks led to a 3D network structure in Q3, which held sufficient ODE to form CdS QD gels.

The X-ray diffraction (XRD) results shown in Fig. 4b illustrated the refractions in the CdS hexagonal phase. The peaks located at  $2\theta = 26.5^\circ$ ,  $44^\circ$ , and  $52^\circ$  could be

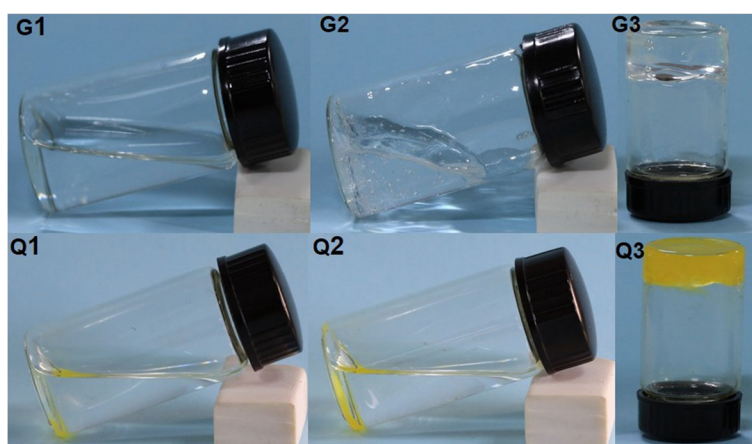


**Fig. 2** Photographs of Cd gelator samples: G1, G2, G3, and the corresponding CdS samples, Q1, Q2, and Q3

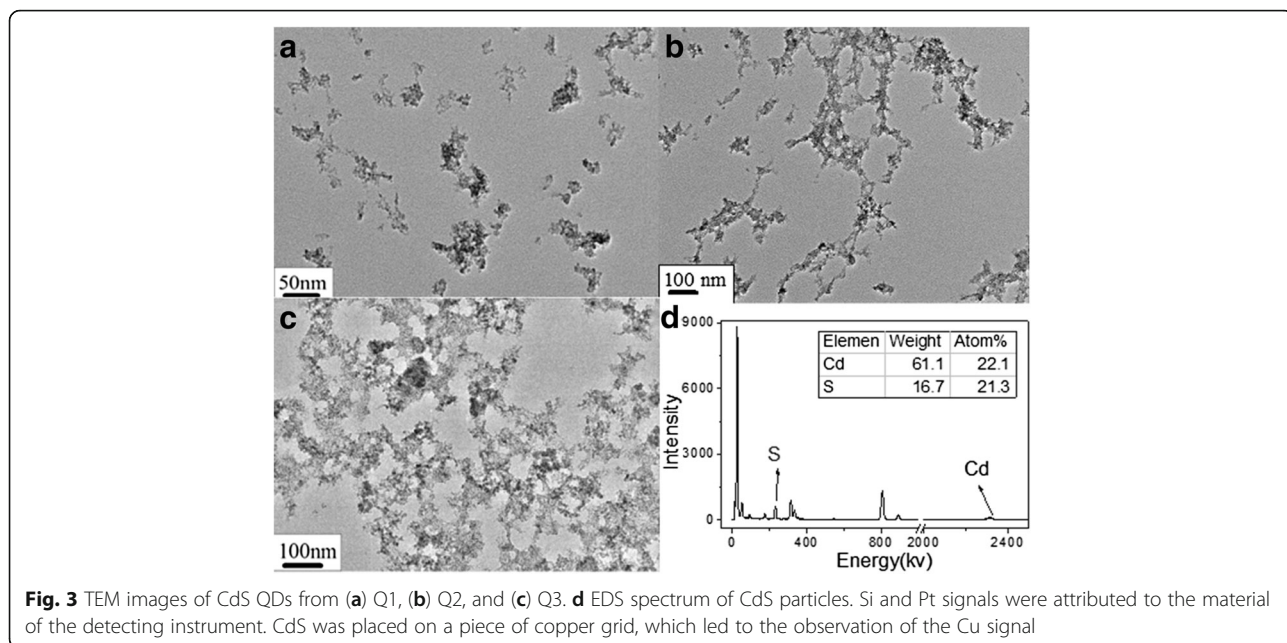


**Fig. 3** TEM images of CdS QDs from (a) Q1, (b) Q2, and (c) Q3. **d** EDS spectrum of CdS particles. Si and Pt signals were attributed to the material of the detecting instrument. CdS was placed on a piece of copper grid, which led to the observation of the Cu signal

indexed to scattering from the (002), (110), and (112) planes, respectively. The peak at 26.5° was deconvoluted into three peaks viz. 24.9(100), 26.5(002), and 28.3(101). The fairly broad peaks confirmed the small particle size.

Macroscopically, apparent differences in color could be observed during the experiments. Compared with the CdS samples Q1 and Q2, the CdS gel Q3 was a darker

color. As shown in Fig. 4c, UV-vis was adopted to investigate the assembly structure of Q2 (curve B) and Q3 (curve A). The UV-visible characterization of these composites revealed the presence of broad absorption bands with absorption maximums ( $\lambda_{max}$ ) at approximately 428 nm (curve A) and 418 nm (curve B). It manifested as a red shift in the UV-vis spectrum, caused by the

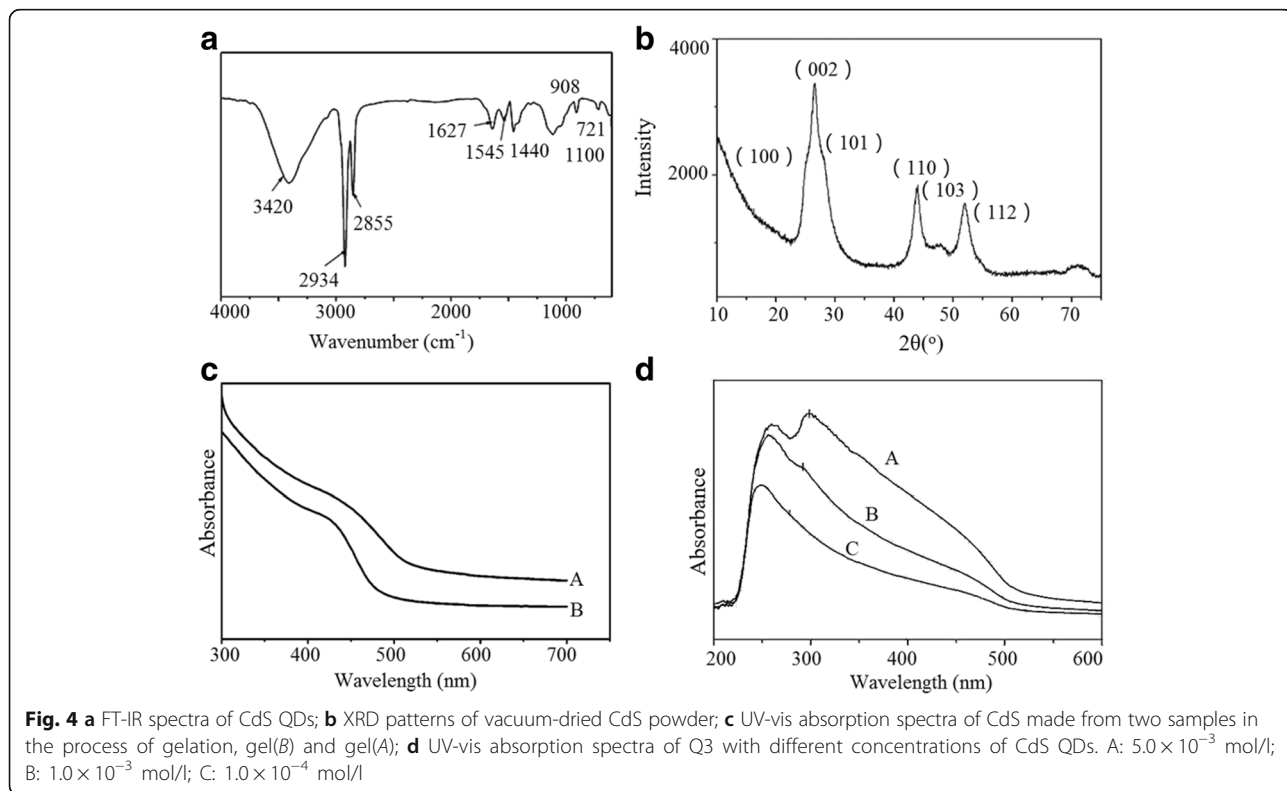


**Fig. 4** **a** FT-IR spectra of CdS QDs; **b** XRD patterns of vacuum-dried CdS powder; **c** UV-vis absorption spectra of CdS made from two samples in the process of gelation, gel(B) and gel(A); **d** UV-vis absorption spectra of Q3 with different concentrations of CdS QDs. A:  $5.0 \times 10^{-3}$  mol/l; B:  $1.0 \times 10^{-3}$  mol/l; C:  $1.0 \times 10^{-4}$  mol/l

formation of network structures. The absorption properties of CdS QDs from several Q3 samples at different concentrations were also investigated. As shown in the UV-vis spectra (Fig. 4d), along with an increase in CdS concentration in toluene, the absorption peak red-shifted from 273 to 301 nm. The peak at around 300 nm was a characteristic absorption of a magic-sized CdS nanocluster. The red shift should be attributed to the aggregation of CdS QDs. This result also proved the existence of the interactions between OA-capped CdS QDs.

The use of QDs as selective fluorescent indicators for inorganic ions assay has been an active research field in analytical chemistry. However, most reports were concerned on the determination of metallic ions by using QDs as probes, few reports related to anion determination especially for the iodate anion. Iodine is an essential micronutrient in human growth. It is of great importance to develop efficient methods to detect iodate in salt and the environmental samples. Although many methods have been proposed, such as resonance scattering spectrometry and ion chromatography, it is still challenging to make the detection limits achieve at  $10^{-8}$  mol/l. Here, it was demonstrated that OA-capped CdS QDs could be used as fluorescent probes to detect iodate anions ( $\text{IO}_4^-$ ). The influence of the pH value on the fluorescence intensity was investigated (Fig. 5a). A phosphoric buffer solution (PBS) was used to keep the system pH value at around 7. The PBS was prepared by adjusting the amounts of  $\text{Na}_2\text{HPO}_4 \cdot 2\text{H}_2\text{O}$  and  $\text{NaH}_2\text{PO}_4 \cdot 2\text{H}_2\text{O}$ . The fluorescence intensity was recorded at 330 nm with an excitation wavelength of 273 nm. By varying the pH from 5.5 to 8.5, it was found that the maximum relative fluorescence intensity ( $F_0/F$ ) appeared at 7.0, where  $F_0$  was the fluorescence intensity of the QDs without quencher and  $F$  was the intensity with the quencher at a certain concentration. The decrease in acid medium might be caused by the protonation of QDs, whereas a high pH might result in the formation of cadmium hydroxide products. A PBS with pH 7 and  $1.0 \times 10^{-5}$  mol/l

of CdS QDs solution (PBS with PH7) was chosen for further experiments.

As shown in Fig. 5b, the fluorescence intensity of CdS QDs was significantly quenched with increasing concentrations of  $\text{IO}_4^-$  in the range from 0.005 to 4.0  $\mu\text{mol/l}$ . The inset of Fig. 5b illustrates the observed good linear relationship between  $F_0/F$  and the concentration of  $\text{IO}_4^-$ . The relationship can be described by the Stern-Volmer equation:

$$F_0/F = 1 + K_{sv}[Q],$$

where  $K_{sv}$  is the Stern-Volmer quenching constant and  $[Q]$  is the concentration of the quencher. The experimental data obtained from  $\text{IO}_4^-$  fitted the following equations:

$$\text{IO}_4^-: F_0/F = 1.0454 + 2.99 \times 10^5 [\text{IO}_4^-],$$

with a correlation coefficient ( $R$ ) of 0.99583.

The limit of detection (LOD) is defined by the equation  $\text{LOD} = 3S_0/K$ , where  $S_0$  is the standard deviation of blank measurements and  $K$  is the slope of the calibration graph. For  $\text{IO}_4^-$ , the LOD was  $3.5 \times 10^{-8}$  mol/l.

Recent studies have tried to find a facile method for constructing NPs into an ordered assembly, especially a method that can stably incorporate the NPs in the networks and form NPs gels. In this study, OA ligated with Cd ions and formed a low-molecule mass gelator of Cd supramolecular gels. By simply introducing sulfur, OA-capped CdS was synthesized in situ. The stabilized layer of OA on the surface of the QDs and the core CdS exactly mirrored the gelators. The in situ formation and the small size of the QDs ensured that the CdS QDs not only retained the 3D network structures of the Cd gels, but also that they existed in gel form. In the obtained CdS gels, the CdS QDs were not assembled along the fiber of the networks, but rather exactly constituted the frameworks. Notably, the formation of the CdS QD gels was greatly influenced by the experimental and environmental parameters (see Additional file 1: Figure S1),

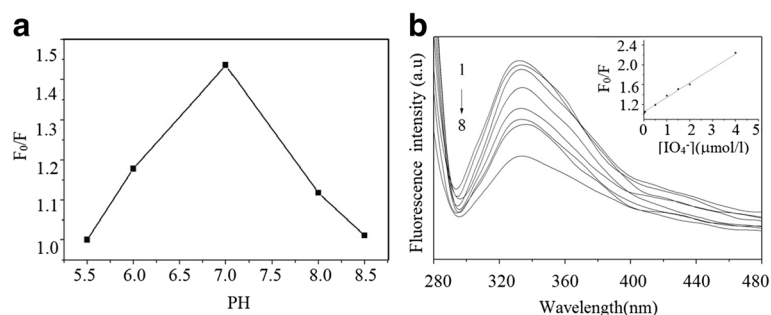


**Fig. 5 a** Influence of pH on the relative fluorescence intensity. CdS QDs:  $1.0 \times 10^{-5}$  mol/l. **b** The fluorescence spectra of CdS QDs in the presence of  $\text{IO}_4^-$  at various concentrations (from 1 to 8): 0, 0.005, 0.05, 0.5, 1.0, 1.5, 2.0, and 4.0  $\mu\text{mol/l}$ . Inset: calibration plots for  $\text{IO}_4^-$

such as the air humidity and H<sub>2</sub>S gas velocity. The new approach developed here points to a new direction for designing proper gelators for further applications. Moreover, we demonstrated that the obtained CdS QDs could be used as fluorescence probes for IO<sub>4</sub><sup>-</sup>. This expands on the applications of previous QDs, which were used in the determination of metallic ions and, rarely, anion determination.

## Conclusion

In summary, a facile one-step method for the in situ synthesis of CdS QD gels at room temperature is presented, using a Cd supramolecular gel as a scaffold. Cd ions from the origin supramolecular gels were used as the precursors of CdS QDs. It was demonstrated that CdS QDs replicated and retained the 3D network structures of the supramolecular gels during the self-assembly process. OA capped on the surface of CdS QDs, not by physical adsorption, but in the form of carboxylate. The resulting QDs can be used as highly sensitive fluorescence probes to detect anions. The present approach offers a new simple method for fabricating QDs with 3D networks, which is a potential route to construct electronic and optical devices.

## Additional file

**Additional file 1: Figure S1.** FT-IR spectra of native gel (red line) and dehydrated solution sample after put in drier for 1 month (black line). (DOCX 70 kb)

## Abbreviations

3D: Three-dimensional; FT-IR: Fourier transform infrared spectroscopy; NPs: Nanoparticles; PBS: Phosphoric buffer solution; QDs: Quantum dots; SAFIN: Self-assembled fibrillar networks; TEM: Transmission electron microscopy; XRD: X-ray diffraction

## Acknowledgements

The authors thank the State Key Laboratory of Coordination Chemistry in Nanjing University for the TEM and XRD analysis, Wei Chen (NJU) for the manuscript modification.

## Funding

This work was supported by the National Natural Science Foundation of China (Grant No. 51133002, 21574063, 51673094, 21304003, and 21404002), the Shenzhen Science and Technology Innovation Committee (JCY20150731091351923, JCY20140903102042989, JCY20160331095239971, JCY20160330095448858, JCY20150806112401354, GJHS20150918111107883), and the Perspective Research Study and Research Alliance of Jiangsu Province of China under Grant (No. BY2014113) for financial support.

## Authors' Contributions

LLZ and JH are co-first authors. LLZ, YW, HCT, and GX designed the experiment. LLZ, HBH, and JH carried out the experiment, as well as wrote the manuscript. CT and LBR were involved in the characterization and analysis of the data, as well as helped to prepare the manuscript. XLW helped to draft and correct the manuscript. All authors read and approved the final manuscript.

## Competing Interests

The authors declare that they have no competing interests.

Received: 15 November 2016 Accepted: 26 December 2016

Published online: 13 January 2017

## References

1. Srivastava S, Kotov NA (2009) Nanoparticle assembly for 1D and 2D ordered structures. *Soft Matter* 5(6):1146–1156
2. Kundu MK, Sadhukhan M, Barman S (2015) Ordered assemblies of silver nanoparticles on carbon nitride sheets and their application in the non-enzymatic sensing of hydrogen peroxide and glucose. *J Mat Chem B* 3(7):1289–1300
3. Thorkelsson K, Bai P, Xu T (2015) Self-assembly and applications of anisotropic nanomaterials: a review. *Nano Today* 10(1):48–66
4. Murray CB, Kagan CR, Bawendi MG (1995) Self-organization of CdSe nanocrystallites into 3-dimensional quantum-dot superlattices. *Science* 270(5240):1335–1338
5. Kobayashi Y, Arai N (2016) Self-assembly of Janus nanoparticles with a hydrophobic hemisphere in nanotubes. *Soft Matter* 12(2):378–385
6. Su HY, Wu CQ, Li DY, Ai H (2015) Self-assembled superparamagnetic nanoparticles as MRI contrast agents - a review. *Chin Phys B* 24(12):11
7. Duan L, Yang F, Song LN, Fang K, Tian JL, Liang YJ, Li MX, Xu N, Chen ZD, Zhang Y, Gu N (2015) Controlled assembly of magnetic nanoparticles on microbubbles for multimodal imaging. *Soft Matter* 11(27):5492–5500
8. Klinkova A, Choueiri RM, Kumacheva E (2014) Self-assembled plasmonic nanostructures. *Chem Soc Rev* 43(11):3976–3991
9. Mertz D, Affolter-Zbaraszcuk C, Barthes J, Cui JW, Caruso F, Baumert TF, Voegel JC, Ogier J, Meyer F (2014) Templated assembly of albumin-based nanoparticles for simultaneous gene silencing and magnetic resonance imaging. *Nanoscale* 6(20):11676–11680
10. Grzybowski BA, Wilmer CE, Kim J, Browne KP, Bishop KJM (2009) Self-assembly: from crystals to cells. *Soft Matter* 5(6):1110–1128
11. Alivisatos AP, Johnsson KP, Peng XG, Wilson TE, Loweth CJ, Bruchez MP, Schultz PG (1996) Organization of 'nanocrystal molecules' using DNA. *Nature* 382(6592):609–611
12. Oaki Y, Imai H (2005) Hierarchically organized superstructure emerging from the exquisite association of inorganic crystals, organic polymers, and dyes: A model approach towards supramineral materials. *Adv Funct Mater* 15(9):1407–1414
13. Yang J, Zeng JH, Yu SH, Yang L, Zhou GE, Qian YT (2000) Formation process of CdS nanorods via solvothermal route. *Chem Mater* 12(11):3259–3263
14. Morales AM, Lieber CM (1998) A laser ablation method for the synthesis of crystalline semiconductor nanowires. *Science* 279(5348):208–211
15. Janczewski D, Tomczak N, Liu SH, Han MY, Vancso GJ (2010) Covalent assembly of functional inorganic nanoparticles by "click" chemistry in water. *Chem Commun* 46(19):3253–3255
16. Jones MR, Macfarlane RJ, Lee B, Zhang JA, Young KL, Senesi AJ, Mirkin CA (2010) DNA-nanoparticle superlattices formed from anisotropic building blocks. *Nat Mater* 9(11):913–917
17. Sun DZ, Gang O (2011) Binary heterogeneous superlattices assembled from quantum dots and gold nanoparticles with DNA. *J Am Chem Soc* 133(14):5252–5254
18. Liu L, Sun CZ, Li ZW, Chen YL, Qian X, Wen SP, Zhang LQ (2016) In-chain functionalized polymer induced assembly of nanoparticles: toward materials with tailored properties. *Soft Matter* 12(7):1964–1968
19. Luo D, Yan C, Wang T (2015) Interparticle forces underlying nanoparticle self-assemblies. *Small* 11(45):5984–6008
20. Zvyagina AI, Ezhov AA, Ivanov VK, Arslanov VV, Kalinina MA (2015) Highly tunable plasmonic assemblies of gold nanoparticles: in-plane manipulation of plasmon coupling with nanometer precision. *J Mater Chem C* 3(45):11801–11805
21. Theis-Brohl K, Gutfreund P, Vorobiev A, Wolff M, Toperverg BP, Dura JA, Borchers JA (2015) Self assembly of magnetic nanoparticles at silicon surfaces. *Soft Matter* 11(23):4695–4704
22. Schreiber R, Do J, Roller EM, Zhang T, Schuller VJ, Nickels PC, Feldmann J, Liedl T (2014) Hierarchical assembly of metal nanoparticles, quantum dots and organic dyes using DNA origami scaffolds. *Nat Nanotechnol* 9(1):74–78
23. Han SC, Hu LF, Gao N, Al-Ghamdi AA, Fang XS (2014) Efficient self-assembly synthesis of uniform CdS spherical nanoparticles-Au nanoparticles hybrids with enhanced photoactivity. *Adv Funct Mater* 24(24):3725–3733
24. Wang ZG, Ding BQ (2014) Engineering DNA self-assemblies as templates for functional nanostructures. *Accounts Chem Res* 47(6):1654–1662

25. Karagoz B, Esser L, Duong HT, Basuki JS, Boyer C, Davis TP (2014) Polymerization-induced self-assembly (PISA) - control over the morphology of nanoparticles for drug delivery applications. *Polym Chem* 5(2):350–355
26. Rycenga M, Camargo PHC, Xia YN (2009) Template-assisted self-assembly: a versatile approach to complex micro- and nanostructures. *Soft Matter* 5(6):1129–1136
27. Ye CH, Meng GW, Wang YH, Jiang Z, Zhang LD (2002) On the growth of CdS nanowires by the evaporation of CdS nanopowders. *J Phys Chem B* 106(40):10338–10341
28. Wu WT, Zhou T, Berliner A, Banerjee P, Zhou SQ (2010) Glucose-mediated assembly of phenylboronic acid modified CdTe/ZnTe/ZnS quantum dots for intracellular glucose probing. *Angew Chem Int Ed* 49(37):6554–6558
29. Braun PV, Osenar P, Tohver V, Kennedy SB, Stupp SI (1999) Nanostructure templating in inorganic solids with organic lyotropic liquid crystals. *J Am Chem Soc* 121(32):7302–7309
30. Sharma KP, AKG, Sen gupta S, Kumaraswamy G (2011) Self-standing three-dimensional networks of nanoparticles with controllable morphology by dynamic templating of surfactant hexagonal domains. *Chem Mater* 23(6): 1448–1455
31. Fu GT, Jiang X, Gong MX, Chen Y, Tang YW, Lin J, Lu TH (2014) Highly branched platinum nanolance assemblies by polyallylamine functionalization as superior active, stable, and alcohol-tolerant oxygen reduction electrocatalysts. *Nanoscale* 6(14):8226–8234
32. Abecassis B (2016) Three-dimensional self assembly of semiconducting colloidal nanocrystals: from fundamental forces to collective optical properties. *ChemPhysChem* 17(5):618–631
33. Wang LH, Zeng Y, Shen AG, Zhou XD, Hu JM (2015) Three dimensional nano-assemblies of noble metal nanoparticle-infinite coordination polymers as specific oxidase mimetics for degradation of methylene blue without adding any cosubstrate. *Chem Commun* 51(11):2052–2055
34. Bals S, Goris B, Liz-Marzan LM, Van Tendeloo G (2014) Three-dimensional characterization of noble-metal nanoparticles and their assemblies by electron tomography. *Angew Chem Int Ed* 53(40):10600–10610
35. Yusuf H, Kim W-G, Lee DH, Alosyna M, Brolo AG, Moffitt MG (2007) A hierarchical self-assembly route to three-dimensional polymer-quantum dot photonic arrays. *Langmuir* 23(10):5251–5254
36. Buerkle LE, Rowan SJ (2012) Supramolecular gels formed from multi-component low molecular weight species. *Chem Soc Rev* 41(18):6089–6102
37. Das D, Kar T, Das PK (2012) Gel-nanocomposites: materials with promising applications. *Soft Matter* 8(8):2348–2365
38. Shen JS, Chen YL, Huang JL, Chen JD, Zhao C, Zheng YQ, Yu T, Yang Y, Zhang HW (2013) Supramolecular hydrogels for creating gold and silver nanoparticles in situ. *Soft Matter* 9(6):2017–2023
39. Weiss RG (2014) The past, present, and future of molecular gels. What is the status of the field, and where is it going? *J Am Chem Soc* 136(21):7519–7530
40. Dong RJ, Pang Y, Su Y, Zhu XY (2015) Supramolecular hydrogels: synthesis, properties and their biomedical applications. *Biomater Sci* 3(7):937–954
41. Sangeetha NM, Maitra U (2005) Supramolecular gels: functions and uses. *Chem Soc Rev* 34(10):821–836
42. Wang XF, Zhang L, Liu MH (2016) Supramolecular gels: structural diversity and supramolecular chirality. *Acta Phys-Chim Sin* 32(1):227–238
43. Du XW, Zhou J, Shi JF, Xu B (2015) Supramolecular hydrogelators and hydrogels: from soft matter to molecular biomaterials. *Chem Rev* 115(24):13165–13307
44. Ono Y, Nakashima K, Sano M, Kanekiyo Y, Inoue K, Hojo J, Shinkai S (1998) Organic gels are useful as a template for the preparation of hollow fiber silica. *Chem Commun* 14:1477–1478
45. Amint M, Ahmad N, Pandey M, Abeer MM, Mohamad N (2015) Recent advances in the role of supramolecular hydrogels in drug delivery. *Expert Opin Drug Deliv* 12(7):1149–1161
46. Kimura M, Kobayashi S, Kuroda T, Hanabusa K, Shirai H (2004) Assembly of gold nanoparticles into fibrous aggregates using thiol-terminated gelators. *Adv Mater* 16(4): 335- +
47. Ray S, Das AK, Banerjee A (2006) Smart oligopeptide gels: in situ formation and stabilization of gold and silver nanoparticles within supramolecular organogel networks. *Chem Commun* 26:2816–2818
48. Love CS, Chechik V, Smith DK, Wilson K, Ashworth I, Brennan C (2005) Synthesis of gold nanoparticles within a supramolecular gel-phase network. *Chem Commun* 15:1971–1973
49. Llusar M, Sanchez C (2008) Inorganic and hybrid nanofibrous materials templated with organogelators. *Chem Mater* 20(3):782–820
50. Bardelang D, Zaman MB, Moudrakovski L, Pawsey S, Margeson JC, Wang DS, Wu XH, Ripmeester JA, Ratcliffe CI, Yu K (2008) Interfacing supramolecular gels and quantum dots with ultrasound: smart photoluminescent dipeptide gels. *Adv Mater* 20(23):4517–4520
51. Xue PC, Lu R, Huang Y, Jin M, Tan CH, Bao CY, Wang ZM, Zhao YY (2004) Novel pearl-necklace porous CdS nanofiber templated by organogel. *Langmuir* 20(15):6470–6475
52. Wu WT, Zhou T, Shen J, Zhou SQ (2009) Optical detection of glucose by CdS quantum dots immobilized in smart microgels. *Chem Commun* 29:4390–4392
53. Simmons B, Li S, John VT, McPherson GL, Taylor C, Schwartz DK, Maskos K (2002) Spatial compartmentalization of nanoparticles into strands of a self-assembled organogel. *Nano Lett* 2(10):1037–1042
54. Shi CS, Zhu J (2007) A solvent-driven organogel shrinkage. *Chem Mater* 19(10):2392–2394

Submit your manuscript to a SpringerOpen<sup>®</sup> journal and benefit from:

- Convenient online submission
- Rigorous peer review
- Immediate publication on acceptance
- Open access: articles freely available online
- High visibility within the field
- Retaining the copyright to your article

---

Submit your next manuscript at ► [springeropen.com](http://springeropen.com)

---